NJC

PAPER

View Article Online
View Journal | View Issue

Cite this: *New J. Chem.*, 2017, 41, 2955

Synthesis and catalytic performance in the propene epoxidation of a vanadium catalyst supported on mesoporous silica obtained with the aid of sucrose

Ewa Janiszewska* and Stanislaw Kowalak

Received 21st November 2016,
Accepted 3rd March 2017

DOI: 10.1039/c6nj03632e

rsc.li/njc

Mesoporous silica was prepared with the use of low-cost and environmentally friendly sucrose as a porogeneous agent. It was found that the presence of sucrose as well as the products of its chemical transformation upon the synthesis procedure (*i.e.*, furfural polymer) affected markedly the structure and morphology of the resulting porous silica. The influences of the sucrose content and the source of the silicon as well as the synthesis conditions (pH, temperature) were very significant. The samples obtained in an acidic medium of the initial mixture formed from TEOS and treated at room temperature gave rise to products with a high surface area and narrow pore size distribution. Despite the lack of pore ordering, their catalytic activity in propene epoxidation after vanadium modification was remarkable in comparison to the activity of the vanadium catalyst supported on ordered mesoporous materials.

Introduction

Mesoporous ordered materials prepared by a surfactant-templated hydrothermal method were first reported in 1992 by Mobil's[1,2] and Toyota's[3] research groups. The high surface area and ordered, uniform pore size (2–50 nm) of this type of material made them a very important group of molecular sieves. Investigations into the synthesis and properties of the mesoporous molecular sieves are still developing enormously due to the potential application of such materials as catalysts, catalyst supports, absorbents, and host materials.[4–6] The great variety of chemical compositions of mesoporous molecular sieves includes also carbon tubes and metallic materials.[4] A large number of various porogeneous materials are applied in many syntheses. Ionic[5–7] or neutral[8–10] surfactants, have been mostly used as templates in the early syntheses of mesoporous materials. Then, di- and triblock copolymers became common and efficient porogeneous agents.[11–13] Many other materials, such as supramolecular aggregates of small molecules,[14] hard templates,[15,16] and even biological matrices, such as virus liquid crystals[17] and plant cellular structures,[18] are currently employed. Sometimes the price of the auxiliary reagents is very high and usually they are not recovered after completed syntheses. Therefore the search for efficient but much less expensive porogeneous materials is still a challenge. The saccharides could be considered worthwhile to check for the synthesis of mesoporous materials. Indeed, there are already some literature reports on the synthesis of mesoporous silica with the aid of carbohydrates as porogeneous agents. The mesoporous silicas were mostly obtained by the sol–gel method in the presence of optically active organic compounds (D-glucose, dibenzoyl-L-tartaric, D-maltose)[19] or hydroxy-carboxylic acids (citric, lactic, malic and tartaric acids)[20] in acidic medium. The synthesis with sucrose as a porogeneous agent, however, has been carried out only in a basic medium.[21] It is assumed that the synthesis of porous silica with these type of porogeneous agents involves hydrogen bonding between the carbohydrate molecules and silanol groups of the silica precursor ($N^{\circ}I^{\circ}$ mechanism), which initiates and directs the formation of the mesostructure. The syntheses were carried out by mixing a carbohydrate solution with silicon source and maintaining the resulting sol at room temperature to allow a slow evaporation of the solvent (for a period of 20 days to 2 months). The mesoporous silicas with a high specific surface area and narrow pore size distribution were obtained after removing the templates by washing or Soxhlet extraction (removal of optically active organic compounds, hydroxy-carboxylic acids) or calcination in air (removal of sucrose). The main drawback of these types of synthesis is their long time. Saccharides were also use in the synthesis of hierarchical materials (AlPO-5, AlPO-11, TS-1)[22,23] to generate mesopores. They were also used as auxiliary agents in the synthesis of ordered mesoporous SBA-1 to enhance its hydrothermal stability.[24,25]

The conditions of the aforementioned synthesis procedures do not noticeably affect the structure of the applied sucrose. It was interesting for us to check if some chemical transformation of sucrose upon the hydrothermal preparation of mesoporous

Adam Mickiewicz University, Faculty of Chemistry, Umultowska 89b, 61614 Poznan, Poland. E-mail: eszym@amu.edu.pl

silica could favorably influence the morphology of the resulting porous products. Hydrothermal synthesis in acidic or basic environment can cause a hydrolysis of carbohydrates with subsequent transformation of the step products toward polymeric products. The latter may play the role of a template in assembling the mesoporous structure. It is conceivable that the obtained porous structure as well as the chemical nature of the surface could be influenced by this approach. The resulting properties could be reflected in an improved efficiency of the catalysts prepared with a silica support when prepared according to the presented procedure.

The ordered mesoporous materials are very often used for the heterogenization of homogeneous catalysts in order to combine the advantages of heterogeneous catalysts, such as an easier product-catalyst separation, with the advantages of homogeneous catalysts, *e.g.* higher selectivity[26–28] as well being used as supports for noble metal or metal oxide catalysts.[29,30] Vanadium oxides supported on mesoporous silica have received much attention because of their catalytic properties. They exhibit high activity and selectivity for a number of reactions, such as the partial oxidation of methane,[31,32] methanol oxidation to formaldehyde,[33,34] and the oxidative dehydrogenation of short-chain alkanes toward the production of the respective alkenes.[35–38] A study on the oxidative dehydrogenation of propane showed that the unique textural properties of these supports allow obtaining very effective and selective catalysts. The high surface area of mesoporous silica allows a better dispersion of metals even at relatively high loadings, compared to classical non-porous or low-surface-area oxide supports.[35,38] Liu *et al.*[38] showed that, not only the high surface area, but also an appropriate structure, pore diameters, or even acidity of silica mesoporous materials can influence the efficiency of the obtained catalysts.

Propylene oxide (PO) is an important intermediate in the production of many fine chemicals. PO is industrially produced by means of two main processes: the chlorohydrin process and by a method that involves organic peroxides. Both processes suffer from serious drawbacks; therefore, the search for new cleaner, more convenient, and safer technologies is still an ongoing challenge. Reviews about different approaches are given by Oyama,[39] Nijhuis,[40] or Cavani *et al.*[41] Although the presented developments were scientifically significant, they suffered from either low PO selectivities, low propylene conversions, or short catalyst lifetimes or they required the use of higher pressures or costly co-reactants. Much attention was paid to propylene epoxidation with H_2O_2 over the TS-1 (MFI) catalyst.[39,41,42] The process involving H_2O_2 was commercialized; however, because of the high price of H_2O_2, the profitability of this process is still an open question.[41] A new perspective in the propene epoxidation process became viable when N_2O was found to be an efficient oxidant along with catalyst based on iron species supported on silica matrices. The epoxidation of propene with N_2O over iron oxide supported on silica and promoted with Na ions attained a propene conversion of ~5–10% at 648 K with a selectivity toward PO of ~50%.[43] It was also shown that various ordered, mesoporous silica materials modified with vanadium species were capable of transforming propene to propylene oxide with a N_2O oxidant. The best results of the investigated series were obtained with catalysts prepared by the impregnation of silica SBA-3 with vanadium ions.[44]

Herein, we present a novel approach to synthesize mesoporous silica with the aid of sucrose by a hydrothermal method. Sucrose, the same as other oligosaccharides, undergoes a hydrolysis in acidic medium to form the respective monosaccharides. The latter can undergo further degradation to heterocyclic aldehydes (furfurals), which readily polymerize and form long chain molecules, suitable for assembling an inorganic material upon condensation. Many earlier studies have indicated that several factors (*e.g.*, temperature, pH, the surfactant/silica ratio, the ions present in the synthesis mixture) could affect the interaction between organic micelles and inorganic species and consequently could influence the final structure of the mesoporous materials during the self-assembly process.[45] As the furfural's polymers are different types of template compared to the conventional neutral templates used for preparing mesoporous materials (*e.g.*, Pluronics), their interaction with silica may differ. For this reason the influence of the source of the silicon, the sucrose content, and the synthesis conditions (pH, temperature) on the properties of the obtained silica samples were examined. The chosen samples of a prepared series with good textural properties (*i.e.*, high surface area, narrow pore size distribution) were used as a support for the vanadium catalyst. Their catalytic ability in the transformation of propene to PO with N_2O as an oxidant was then evaluated.

Experimental

Synthesis

Water glass (WG, $Na_2O/SiO_2/H_2O$ = 15.25/30/54.75 in wt%, Vitrosilicon, Poland) and tetraethoxysilane (TEOS, Aldrich) were the principal sources of silicon applied for the syntheses. Sucrose (POCh, Poland) was used as the porogeneous agent (PA). The pH of the gel was adjusted in the range of 1–12 by adding adequate amounts of aqueous ammonia (POCh, Poland) or hydrochloric acid (POCh, Poland). In a typical synthesis, the solution of sucrose (40 wt%) was mixed with the solution containing the silicon source. The pH of the mixture was then adjusted to the chosen value. The mixture was stirred at room temperature for 2 h and then heated (if necessary) in the temperature range 298–443 K for 20 h. The resulting products were filtered, washed with distilled water, dried, and calcined in air (723–973 K) to remove the organic components.

A support with the SBA-3 structure was synthesized as a benchmark matrix for the vanadium catalysts. It was obtained according to the literature description with cetyltrimethylammonium bromide (CTABr, Aldrich) and tetraethylorthosilicate (TEOS, Aldrich) as the principal reagents.[46]

Characterization

The products were characterized by means of standard methods. The characterization procedures comprised the calcined samples as well as those obtained right after the hydrothermal syntheses. X-ray diffraction (XRD) patterns were collected using a Bruker D8

Advance diffractometer with Cu-Kα radiation (λ = 1.54056 Å). Fourier transform infrared spectra (KBr) were recorded with a Bruker Vector 22 spectrophotometer. Transmission electron microscopy (TEM) images were taken using HRTEM with a JEOL ARM 200F instrument operating at 200 kV. The thermal behavior of the samples was followed by thermogravimetric and differential thermal analyses (TG and DTA) in air (with a heating rate of 10 °C min^{-1}) using SETARAM SETSYS 12 equipment. The BET surface area and pore parameters of the samples were determined by nitrogen adsorption–desorption isotherm measurements at 77 K on a Micromeritics ASAP 2000 sorptometer. The samples were outgassed at 573 K prior to the measurement. The total pore volume and average pore radius were determined by the Barrett–Joyner–Halenda (BJH) method. UV-vis diffuse reflectance spectra of the vanadium-modified samples were recorded at room temperature on a Cary 100 UV-vis spectrometer (Varian) in the range of 190–900 nm. Prior to measurement, the samples were diluted with the pure silica (SiO_2, POCh, Poland) with the weight ratio of 1 : 100 and were then dehydrated by calcination for 1 h at 673 K. The spectrum of the silica support was subtracted as the baseline for each catalyst.

Catalyst preparation and catalytic studies

The chosen samples were modified with vanadium ions by means of incipient wetness impregnation, using aqueous solutions of $VOSO_4 \cdot 5H_2O$ (in an amount related to 3 wt% of V). After impregnation and drying (373 K), the catalysts were calcined in air at 823 K for 1 h.

The catalytic tests for propene oxidation were performed in a continuous flow reactor. Catalytic experiments were carried out at 653 K, under atmospheric pressure, with WHSV = 3420 ml h^{-1} g_{cat}^{-1}, related to a contact time of 1.1 s. Prior to the measurements, the catalysts were heated in a helium flow at 723 K for 30 min. The substrates, propene and N_2O, were diluted with helium (molar ratio of propene : nitrous oxide : helium = 1 : 15 : 12.5). The products were analyzed using on-line GC, equipped with FID and TCD detectors. The catalytic performances were expressed in terms of conversion (%), selectivity (%), and yield (%), calculated as described elsewhere.[44]

The catalytic activity of the samples was compared with the activity of vanadium catalyst supported on conventional silica SBA-3. SBA-3 silica has already been studied in our laboratory as a matrix of the vanadium catalyst for propylene epoxidation and was found to be the most promising silica support among several other under study.[44]

Results and discussion

Synthesis

Synthesis in a basic medium (pH = 12) of the initial mixture allowed obtaining only a small amount of the solid product; whereas a much higher yield was obtained when the synthesis was conducted at lower pH (8 or particularly 1). It is well known that the silica precursor can form different species under different pH. When the synthesis is performed in a basic medium, the stable

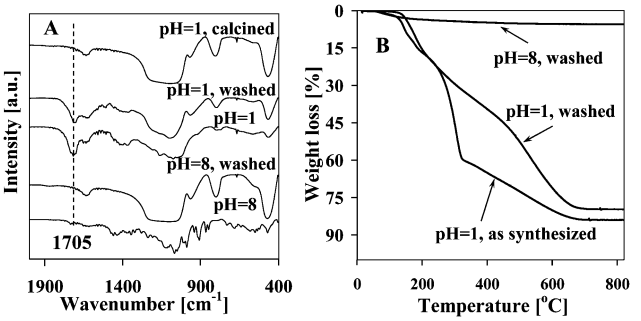

Fig. 1 FTIR spectra (A) and weight loss (TG) (B) for the samples synthesized at the indicated pH (water glass, PA/Si = 1.69, 368 K).

dimeric silicic species exist in solution and only weakly interact with the template and do not polymerize to form a continuous regular network.[45]

It was interesting to note that synthesis in acidic medium (pH = 1) caused a formation of a dense dark brown jelly. The transparent jelly was formed from almost neutral (pH = 8) mixtures on heating, as well as from acidic mixtures at ambient temperature (RT). The brown color of the samples obtained in acidic medium at elevated temperature was caused by the condensation of furfural formed during the hydrolysis of sucrose and its subsequent transformation. The presence of furfural or the product of its polymerization could be seen in the FTIR spectra of the samples obtained in an acidic medium (at RT and elevated temperatures) as a band at *ca.* 1700 cm^{-1} (C═O band), which disappeared after calcination (Fig. 1A). This band could be seen both in the spectra of the as-synthesized samples as well in the spectra of the washed samples, which suggests that the water insoluble furfural polymer is a prevailing organic material embedded in the resulting porous silica. If monomeric furfural were present in the samples, the band at 1700 cm^{-1} then vanished on washing (solubility of furfural in water is 83 g l^{-1}).

The formation of insoluble furfural polymer was confirmed by thermal analysis (TG). The weight loss on calcination of the samples synthesized in acidic medium was high (*ca.* 80%). A very similar weight loss could also be seen for the as-synthesized samples after washing. Samples obtained at almost neutral pH showed a low weigh loss (*ca.* 5%) after washing, which suggests that water soluble organic compounds (*i.e.*, furfural) can be removed from the products (Fig. 1B). This was also reflected in vanishing of the band at 1700 cm^{-1} in the FTIR spectra of the samples synthesized at pH = 8 after washing.

The thermal analysis of the samples indicated two distinct steps in weight loss on heating (TG curves) (Fig. 2). The first one (up to *ca.* 300 °C) results from removal of water, which is consistent with the respective endothermic effect (DTA curves). The next significant weight loss (200–600 °C) is due to the organic compounds decomposition. The DTA curves show exo- and endothermic effects in this region, which can originate from oxidation of the organic compounds and desorption of the oxidation products, respectively. In the case of samples obtained from TEOS, additional exo- and endothermic effects

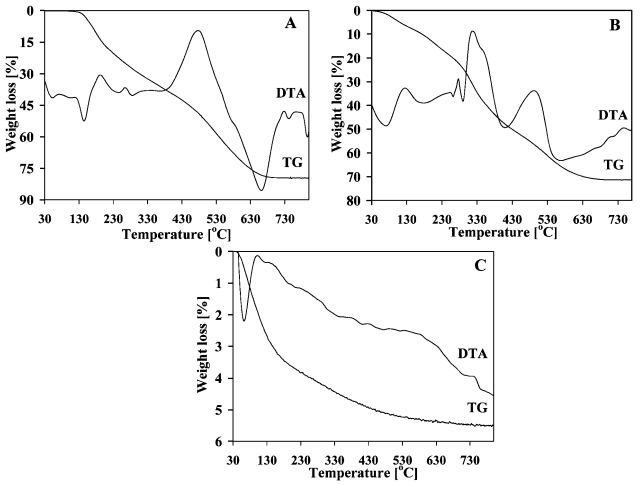

Fig. 2 TG and DTA analyses of the washed samples synthesized under the indicated conditions: water glass, PA/Si = 1.69, 368 K (pH = 1 (A), pH = 8 (C)); TEOS, PA/Si = 0.56, pH = 1, 368 K (B).

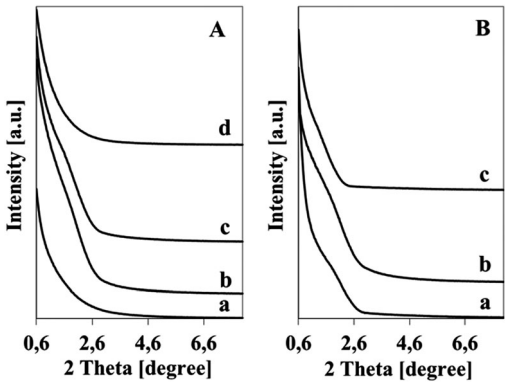

Fig. 3 Low-angle XRD patterns of the samples obtained with different sources of silica: (A) water glass (pH = 1, 368 K, PA/Si = 0.38 (a), PA/Si = 0.56 (b), PA/Si = 1.69 (c); pH = 8, 368 K, PA/Si = 1.69 (d)); (B) TEOS (pH = 1, PA/Si = 0.56, 298 K (a), 368 K (b), 443 K (c)).

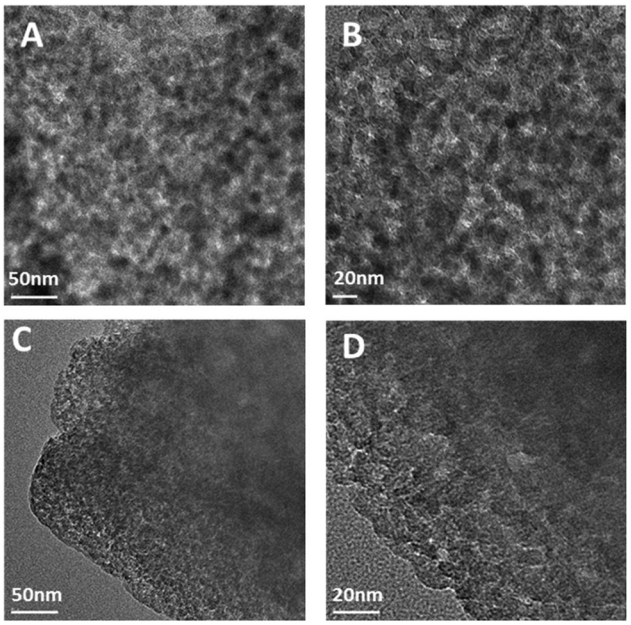

Fig. 4 TEM micrographs of the samples obtained from water glass ((A and B) pH = 1, PA/Si = 1.69, 368 K) and TEOS ((C and D) pH = 1, PA/Si = 0.56, 368 K).

in the temperature range of 250–450 °C are observed. This can be attributed to the oxidation and desorption of some not completely reacted TEOS (remaining ethoxy groups)[47] or from compounds that might be generated from ethanol and furfural derivatives during the synthesis. The washed samples formed at pH ~ 8 indicate a low weight loss during the calcination and that it takes place within the whole investigated temperature range. The predominant endothermic effect on the DTA curve (at ~100 °C) results from desorption of the adsorbed water. The further weight loss is probably caused by dehydration of the silanol groups. Contrary to the above samples (Fig. 2A and B), there was no evidence of any thermal effects on the DTA curve due to a decomposition or transformation of organic remnants.

Ordering of the pore system in the samples

XRD patterns in the high angle region (6–60°) of all samples (not shown) indicate only a broad halo at a 2Θ value of ~23°, which corresponds to amorphous silica and confirms the amorphous nature of the samples under study. The low-angle powder XRD patterns show only a shoulder (small intensity broad peak), which could indicate some, but rather poor, ordering of mesopores in the short range (Fig. 3). The samples obtained with a low amount of saccharide or at higher pH did not show even this shoulder.

TEM micrographs confirmed a lack of long-range order in the pore structures. However, for some samples, interconnected worm-like pores (Fig. 4) with disordered arrangements are displayed in the images.[48] The TEM images of the presented samples look similar to those prepared with the contribution of sucrose and presented in the literature.[19,47,48]

Textural characterization

The obtained samples exhibited IV-type adsorption–desorption isotherms. This type of isotherm always indicates the presence of mesopores in the obtained samples. The surface area value and pore size distribution depend markedly on the synthesis parameters (Table 1). In general, an increase in sucrose content (in respect to silicon) in the initial mixture resulted in an increasing BET surface area (samples 1, 2, 3). Such a correlation was also observed for the mesoporous materials prepared with the aid of nonsurfactant templates.[19–21] Moreover, the increase in the template concentration resulted in a reduced average pore size (Fig. 5A). The latter is in contrast to previously observed correlations.[19,20] Also, the pore size distribution became even more uniform with increasing the amount of sucrose. Samples synthesized with a higher amount of sucrose showed a narrow pore size distribution in a range from 2 to 9 nm and similar isotherms, with a steep rise in the adsorbed volume at a relative pressure of $p/p_0 > 0.4$. The hysteresis loop in the partial pressure region from 0.4 to 0.8 implies framework mesoporosity.[49] The sample obtained with the lowest amount

Table 1 Textural properties of the chosen samples

Sample number	Si source	PA/Si	Initial pH of synthesis	Temp. of synthesis [K]	Surf. area [m^2 g^{-1}]	Mean pore diam. [nm]	Pore volume [cm^3 g^{-1}]
1	Water glass	0.38	1	368	431	7.5	0.81
2	Water glass	0.56	1	368	524	5.0	0.66
3	Water glass	1.69	1	368	599	4.8	0.72
4	Water glass	1.69	8	368	230	17.9	1.03
5	TEOS	0.56	1	368	607	4.0	0.61
6	TEOS	0.56	8	368	177	19.1	0.84
7	Water glass	1.69	1	298	559	3.5	0.49
8	Water glass	1.69	1	443	381	12.6	1.20
9	TEOS	0.56	1	298	808	3.0	0.60
10	TEOS	0.56	1	443	247	17.6	1.08

of sucrose showed an isotherm with a steep rise in the adsorbed volume at a relative pressure of $p/p_0 > 0.8$, corresponding to a relatively larger pore size (above 10 nm) and a broader pore size distribution (3 to 30 nm) than the other samples. According to the literature, a hysteresis loop at high partial pressure ($p/p_0 > 0.8$) is indicative of textural mesoporosity and/or macroporosity, whereas a sharp increase in nitrogen uptake at $p/p_0 > 0.9$ is indicative of a significant amount of interparticle mesoporosity.[49] Therefore, the porosity of this sample most likely arises from voids formed between the aggregated particles. These results indicate that the presence of a certain amount of sucrose in the initial gel is important for the formation of a uniform mesoporous structure. Too low a content of sugar in the mixture results in only a limited amount of the silicon participating in the inorganic–organic assembling process, which results in a low surface area.

Lowering the pH of the initial mixture (samples 3, 4 and 5, 6) resulted in a higher surface area, lower average pore size, and more narrow pore size distribution in the resulting samples (Fig. 5B). The increase in nitrogen uptake at $p/p_0 > 0.9$ for samples obtained at higher pH indicated only the presence of interparticle mesoporosity. Usually, changes in the textural properties of materials with an increase of the pH of the synthesis mixture can be explained by the changes in the formation mechanism and the rate of hydrolysis and polymerization of the inorganic source.[45,50] Here though, the absence of framework porosity in the presented synthesis at higher pH could results from the fact that furfural polymer is not formed, while the monomeric furfural formed in these conditions is unable to form mesopores in the silica framework. The broadening of the pore size distribution at a higher pH of the synthesis mixture is in line with previously reported results, in which different surfactants and silica precursors were used.[45,50–52] This is caused by the increasing silica dissolution–reprecipitation processes that take place with increasing pH values and also the weaker interactions between the oligomeric silicic species and the template.

Syntheses with TEOS instead of water glass (sample 2 and 5) under the same conditions (the same pH, temperature, molar ratio PA/Si) led to products with a higher surface area and narrower pore size distribution (Fig. 5C). According to the literature data, inorganic species (*e.g.*, Na^+) present in synthesis mixture can interact with surfactants and change the specific interaction between the surfactant and silica species, thus improving the properties of the obtained materials (better ordering, shape of crystals, *etc.*) or lowering the temperature of synthesis.[53,54] Using a cheap sodium silicate instead of TEOS for the synthesis of SBA materials does not affect the formation of well-ordered samples with good textural properties.[55,56] In our case, sodium cations present in water glass could change the mechanism of mesoporous silica formation to be less favorable. Probably the interactions between the template and silica are weaker than in the case when TEOS was used as a silica source. A similar observation was also reported by Léonard *et al.*[45]

Regardless of the silica source, lowering the temperature of synthesis seems beneficial for obtaining a high porosity of the products (samples 7, 3, 8 or 9, 5, 10). The samples obtained at room temperature had a higher surface area, relatively small average pore size, and narrower pore size distribution than those prepared at elevated temperatures (Fig. 5D). With increasing the temperature of synthesis the steep rise in the adsorbed volume is shifted to a higher value of relative pressure p/p_0 and the contribution of framework mesoporosity decreases. The higher temperature also favors the formation of a less uniform pore size distribution and increased pore size. Similar observations are reported in the literature for mesoporous materials obtained in the presence of neutral surfactants.[51,57] This is caused by the increased radius of the micelles[51] or weakened H-bonds between the surfactant head groups and the neutral inorganic precursor species with an increasing temperature of synthesis.[57] A decrease in the framework porosity and its absence for the samples synthesized at 443 K, as observed in the presented results, suggests that the condensation of silica at this temperature is too fast in comparison to the rate of furfural resin formation and that it takes place practically without participation of the template. The increasing pore size value and pore volume are only a result of the existing silica interparticle porosity.

Catalytic properties

The chosen samples with the best textural properties (samples 9 and 5 obtained in acidic medium with TEOS as a silicon source at 298 and 368 K) were applied for the accommodation of vanadium species and were employed as catalysts for propene epoxidation with N_2O as an oxidant. The samples differed slightly in surface area and pore diameter, which could influence

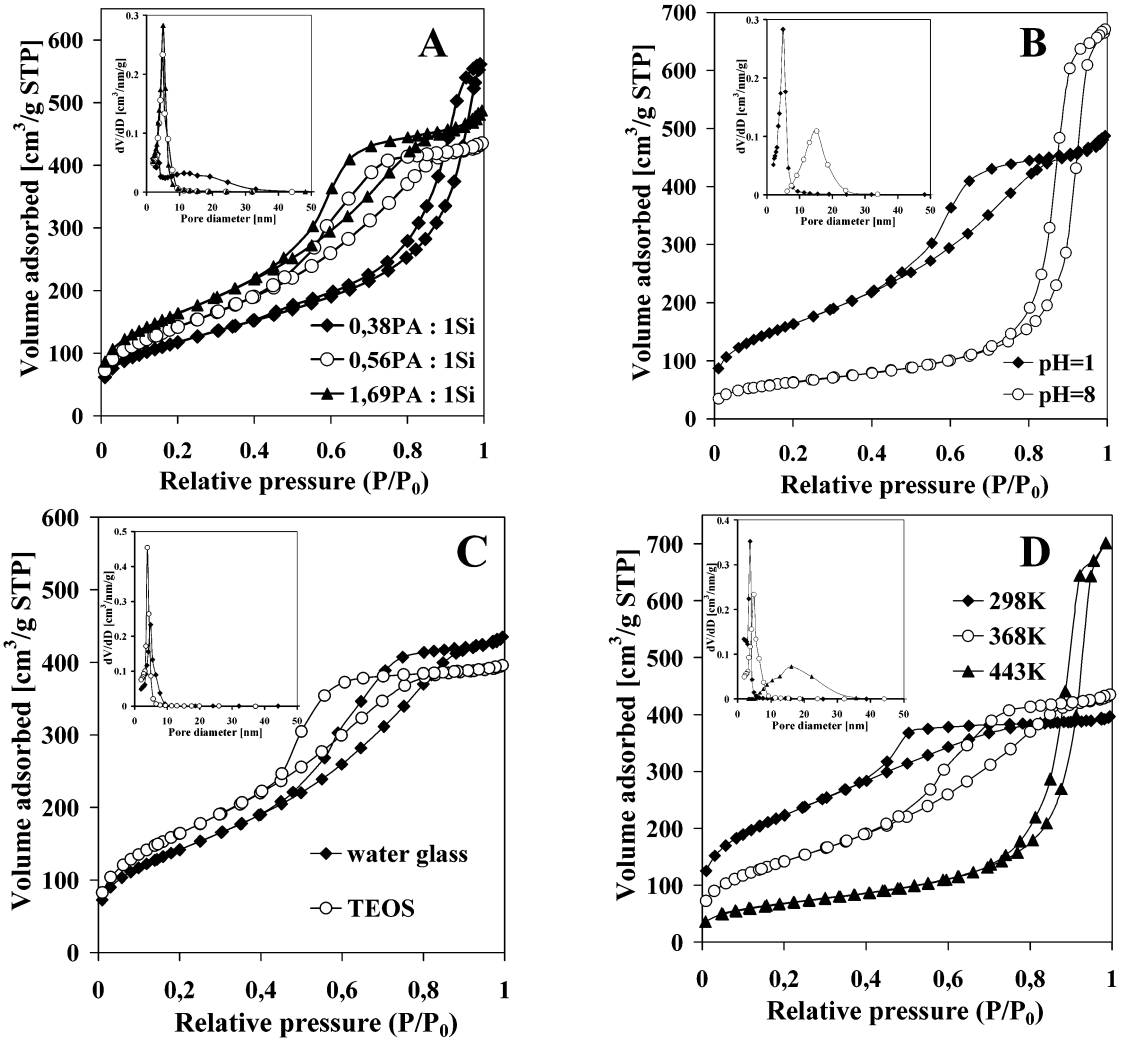

Fig. 5 N_2 adsorption–desorption isotherms for samples synthesized: (A) with different concentration of sucrose (water glass, pH = 1, 368 K), (B) at different pH (water glass, PA/Si = 1.69, 368 K), (C) with different source of silicon (PA/Si = 0.56, pH = 1, 368 K), (D) at different temperatures (TEOS, PA/Si = 0.56, pH = 1). The insets represent pore size distributions.

the distribution and kind of formed vanadium species on their surface.

It was found that the surface area and pore volume of the vanadium-impregnated materials decreased in comparison to the unmodified samples, whereas the pore diameters did not change (Table 2). This indicates, that the formed vanadium species were located only inside the pores or on the surface.

The vanadium-modified samples showed activity for propylene epoxidation (Fig. 6). Besides the desired propylene oxide, several other oxidation products, mainly propionaldehyde, acetone, acrolein, and CO_x, are always found in the reaction products. The vanadium-modified samples obtained on the support synthesized at room temperature showed noticeable propene conversion and PO yields in comparison to the activity of the vanadium catalyst supported on SBA-3 silica. The catalyst obtained from the silica sample synthesized at elevated temperature exhibited a much lower activity in the studied reaction. The significant differences observed in the activity and the selectivity to PO result from the different kinds of vanadium species formed on the surfaces of the used materials. UV-vis spectra recorded for the catalysts diluted with SiO_2 and as dehydrated exhibit absorption bands at 4.0, 4.9, and 5.8 eV (Fig. 7). These bands are attributed to the ligand-to-metal charge-transfer (CT) of T_d-coordinated V^{5+} species. The band at 5.8 eV is assigned to highly dispersed, monomeric tetrahedrally coordinated VO_x species. The additional band at 4.0 eV is attributed to oligomeric

Table 2 Textural properties of the supports and catalysts

Sample	Temp. of synthesis [K]	Surf. area [$m^2\ g^{-1}$]	Mean pore diam. [nm]	Pore volume [$cm^3\ g^{-1}$]
SBA-3	298	1432	2.1	0.74
3V/SBA-3		1144	2.0	0.56
9	298	808	3.0	0.60
3V/9		663	3.0	0.50
5	368	607	4.0	0.61
3V/5		522	4.1	0.54

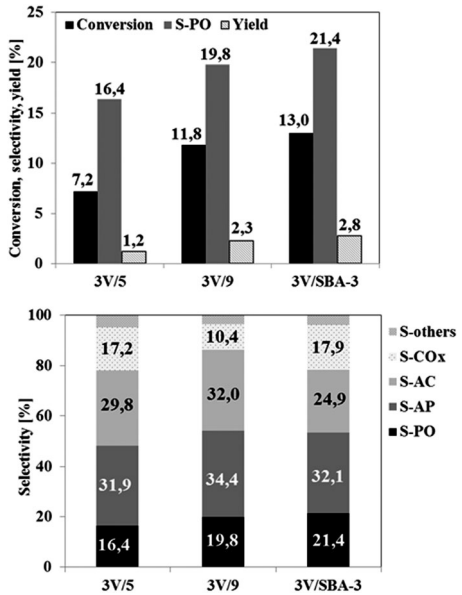

Fig. 6 Propylene conversion, selectivity to PO, and PO yield (top), and selectivity toward all the products (bottom) for the indicated samples at 653 K (PO – propylene oxide, AP – propionaldehyde, AC – acetone + acrolein, CO_x – CO + CO_2).

tetrahedral VO_x groups linked in the chains by V–O–V bridges. The band at 4.9 eV is common for both isolated monomeric and oligomeric tetrahedrally coordinated VO_x species.[58] The band assigned to T_d oligomers for the samples obtained at elevated temperature is divided into two bands (at 3.99 and 3.61 eV), probably due to the different lengths of oligomeric V^{5+} species. This sample exhibits also a higher amount of oligomeric tetrahedral V^{5+} species in comparison to the samples obtained at 298 K (Table 3). The sample obtained at 298 K shows almost exclusively the isolated V^{5+} species in the tetrahedral position (similar to the vanadium-modified SBA-3 material), which is in contrast to the sample obtained at elevated temperature (Table 3). According to the literature data,[44] this type of vanadium species is responsible for catalytic activity in propene epoxidation. This explains the higher activity of the sample obtained at room temperature. The obtained results indicated that a higher surface area (*e.g.*, for the sample obtained at 298 K) provides a better distribution of vanadium moieties and leads to the formation of

Table 3 Results of the UV-vis spectra data for the vanadium-modified samples

Sample	Temp. of synthesis [K]	UV-vis band position [eV]	Area of absorption band	VO_x structure
3V/SBA-3	298	4.93	0.2624	T_d, mono + oligo
		5.81	0.0714	T_d, mono
3V/9	298	4.13	0.0024	T_d, oligo
		4.93	0.2619	T_d, mono + oligo
		5.80	0.0652	T_d, mono
3V/5	368	3.61	0.0084	T_d, oligo
		3.99	0.0358	T_d, oligo
		4.90	0.2980	T_d, mono + oligo
		5.80	0.0734	T_d, mono

mostly isolated V^{5+} species, which are efficient in catalytic reactions. The formation of a higher amount of bigger vanadium species on the sample obtained at elevated temperature could be caused by the lower surface area in comparison to the surface area of the sample synthesized at 298 K. The vanadium catalyst based on the silica support synthesized at 298 K showed a lower activity than that obtained with the SBA-3 support, despite the same nature of the vanadium sites (isolated monomeric VO_x). The reason for the lower activity may result from its larger pores (3.0 nm) in comparison to the pores of the SBA-3 support (2.0 nm). Such an observation was also made by Pérez-Ramírez *et al.*[59] The authors examined the catalytic activity of microporous Fe–silicalite and mesoporous Fe-SBA-15 with very similar amounts, nature, distribution, and redox properties of the extra framework iron species. They suggested that the large pores in SBA-15 did not generate the required intimate contact between the potentially active Fe sites and the reactant molecules, with most of the latter just passing through the pore system of mesoporous silica without approaching the active sites. Perhaps in the case of our catalyst with larger pores (prepared with the contribution of furfural), its lower activity compared to the narrower SBA-3 also results from a retarded contact of reagents with the vanadium active sites. The lowest activity of the catalyst with the support prepared at elevated temperature could be caused not only by the lower number of active V monomers but also by a limited contact with them, even in the case of the larger pore system (4.0 nm).

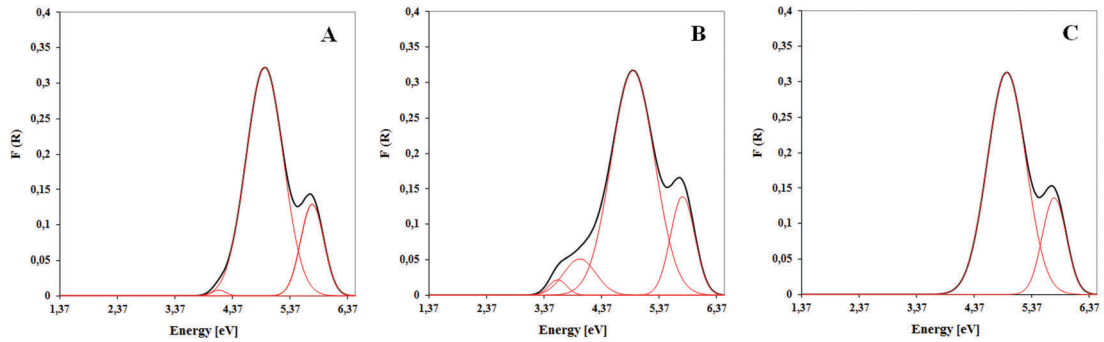

Fig. 7 UV-vis reflectance spectra of diluted samples of vanadium catalysts supported on silica obtained at 298 K (A), 368 K (B), and SBA-3 (C).

Conclusions

The presented results indicate that sucrose can be used as an efficient porogeneous agent for the preparation of porous silica. The interaction of sucrose with silicon precursors by means of hydrogen bonds suggested in earlier works[19,21] is very likely. However, the most spectacular influence of sucrose on the properties of the resulting porous silica was noticed in acidic medium, which facilitated hydrolysis of the disaccharide, and, moreover, it initiated the transformation to furfural and subsequent polymerization. It is likely that the formed polymer chains interact with silicic acid, resulting in assembly of the silica tetrahedra upon their condensation around the furfural polymer matrix. Such an action of furfural polymers could be responsible for the formation of silica porous materials with a high surface area and relatively narrow mesopore size distribution. Similarly, as reported in the syntheses of porous silica with the aid of saccharose,[21] the obtained samples did not exhibit pore ordering, as is always noticed for typical M41S or SBA materials. The presented preparation procedure is not energy and time-consuming (room temperature, 20 h) and given the very low cost of sucrose (contrary to conventional templates) could gain practical significance. It is likely that further optimization of the synthesis may lead to products with a tailored porous structure and the desired nature of the surface. The vanadium-modified samples showed a noticeable activity and selectivity in propylene epoxidation and it is possible that further study could bring more promising results.

Acknowledgements

This work was supported by National Science Centre (grant no. N N204 119238). The authors thank Dr Agnieszka Held (Faculty of Chemistry, Adam Mickiewicz University, Poznan) for catalytic activity examination and Dr Grzegorz Nowaczyk (NanoBioMedical Centre, Adam Mickiewicz University, Poznan) for the HR-TEM measurements.

References

1 C. T. Kresge, M. E. Leonowicz, W. J. Roth, J. C. Vartuli and J. S. Beck, *Nature*, 1992, **359**, 710–712.
2 J. S. Beck, J. C. Vartuli, W. J. Roth, M. E. Leonowicz, C. T. Kresge, K. D. Schmitt, C. T.-W. Chu, D. H. Olson, E. W. Sheppard, S. B. McCullen, J. B. Higgins and J. L. Schlenker, *J. Am. Chem. Soc.*, 1992, **114**, 10834–10843.
3 T. Yanagisawa, T. Shimizu, K. Kuroda and C. Kato, *Bull. Chem. Soc. Jpn.*, 1990, **63**, 988–992.
4 R. Xu, W. Pang, J. Yu, Q. Huo and J. Chen, *Chemistry of Zeolites and Related Porous Materials: Synthesis and Structure*, J. Wiley & Sons (Asia) Pte Ltd, Singapore, 2007.
5 A. D. Firouzi, D. Kumar, L. M. Bull, T. Besier, P. Sieger, Q. Huo, S. A. Walker, J. A. Zasadzinski, C. Glinka, J. Nicol, D. Margolese, G. D. Stucky and B. F. Chmelka, *Science*, 1995, **267**, 1138–1143.
6 Q. Huo, R. Leon, P. M. Petroff and G. D. Stucky, *Science*, 1995, **268**, 1324–1327.
7 D. Danino, Y. Talmon and R. Zana, *Langmuir*, 1995, **11**, 1448–1456.
8 P. T. Tanev, M. Chibwe and T. J. Pinnavaia, *Nature*, 1994, **368**, 321–323.
9 S. A. Bagshaw, E. Prouzet and T. J. Pinnavaia, *Science*, 1995, **269**, 1242–1244.
10 W. Zhang, M. Froeba, J. Wang, P. T. Tanev, J. Wong and T. J. Pinnavaia, *J. Am. Chem. Soc.*, 1996, **118**, 9164–9171.
11 D. Zhao, J. Feng, Q. Huo, N. Melosh, G. H. Fredrickson, B. F. Chmelka and G. D. Stucky, *Science*, 1998, **279**, 548–552.
12 D. Zhao, Q. Huo, J. Feng, B. F. Chmelka and G. D. Stucky, *J. Am. Chem. Soc.*, 1998, **120**, 6024–6036.
13 G. D. Stucky, D. Zhao, P. Yang, W. Lukens, N. Melosh and B. F. Chmelka, *Stud. Surf. Sci. Catal.*, 1998, **117**, 1–12.
14 S. Polarz, B. Smarsly, L. Bronstein and M. Antonietti, *Angew. Chem., Int. Ed.*, 2001, **40**, 4417–4421.
15 R. Ryoo, S. H. Joo and S. Jun, *J. Phys. Chem. B*, 1999, **103**, 7743–7746.
16 F. Schüth, *Angew. Chem., Int. Ed.*, 2003, **42**, 3604–3622.
17 C. E. Fowler, W. Shenton, G. Stubbs and S. Mann, *Adv. Mater.*, 2001, **13**, 1266–1269.
18 Y. Shin, J. Liu, J. H. Chang, Z. Nie and G. J. Exarhos, *Adv. Mater.*, 2001, **13**, 728–732.
19 Y. Wei, D. Jin, T. Ding, W.-H. Shih, X. Liu, S. Z. D. Cheng and Q. Fu, *Adv. Mater.*, 1998, **4**, 313–316.
20 J.-B. Pang, K.-Y. Qiu, Y. Wie, X.-J. Lei and Z.-F. Liu, *Chem. Commun.*, 2000, 477–478.
21 D.-W. Lee, Ch.-Y. Yu and K.-H. Lee, *J. Mater. Chem.*, 2009, **19**, 299–304.
22 X. Yang, T. Lu, Ch. Chen, L. Zhou, F. Wang, Y. Su and J. Xu, *Microporous Mesoporous Mater.*, 2011, **144**, 176–182.
23 W. Wang, G. Li, L. Liu and Y. Chen, *Microporous Mesoporous Mater.*, 2013, **179**, 165–171.
24 Ch.-Ch. Ting, H.-Y. Wu, Y.-Ch. Pan, S. Vetrivel, G. T. K. Fey and H.-M. Kao, *J. Phys. Chem. C*, 2010, **114**, 19322–19330.
25 H.-M. Kao, Ch.-Ch. Ting, A. S. T. Chiang, Ch.-Ch. Teng and Ch.-H. Chen, *Chem. Commun.*, 2005, 1058–1060.
26 A. Corma and H. Garcia, *Chem. Rev.*, 2002, **102**, 3837–3892.
27 D. E. De Vos, M. Dams, B. F. Sels and P. A. Jacobs, *Chem. Rev.*, 2002, **102**, 3615–3640.
28 S. Koner, K. Chaudhari, T. K. Das and S. Sivasanker, *J. Mol. Catal. A: Chem.*, 1999, **150**, 295–297.
29 D. T. On, D. Desplantier-Giscard, C. Danumah and S. Kaliaguine, *Appl. Catal., A*, 2003, **253**, 545–602.
30 A. Taguchi and F. Schüth, *Microporous Mesoporous Mater.*, 2005, **77**, 1–45.
31 H. Berndt, A. Martin, A. Brückner, E. Schreier, D. Müller, H. Kosslick, G.-U. Wolf and B. Lücke, *J. Catal.*, 2000, **191**, 384–400.
32 L. D. Nguyen, S. Loridant, H. Launay, A. Pigamo, J. L. Dubois and J. M. M. Millet, *J. Catal.*, 2006, **237**, 38–48.
33 M. Baltes, K. Cassiers, P. Van Der Voort, B. M. Weckhuysen, R. A. Schoonheydt and E. F. Vansant, *J. Catal.*, 2001, **197**, 160–171.

34 M. Baltes, P. Van Der Voort, O. Collart and E. F. Vansant, *J. Porous Mater.*, 1998, **5**, 317–324.
35 S. A. Karakoulia, K. S. Triantafyllidis and A. A. Lemonidou, *Microporous Mesoporous Mater.*, 2008, **110**, 157–166.
36 L. Čapek, J. Adam, T. Grygar, R. Bulánek, L. Vradman, G. Košová-Kučerová, P. Čičmanec and P. Knotek, *Appl. Catal., A*, 2008, **342**, 99–106.
37 R. Zhou, Y. Cao, S. Yan, J. Deng, Y. Liao and B. Hong, *Catal. Lett.*, 2001, **75**, 107–112.
38 Y.-M. Liu, W.-L. Feng, T.-Ch. Li, H.-Y. He, W.-L. Dai, W. Huang, Y. Cao and K.-N. Fan, *J. Catal.*, 2006, **239**, 125–136.
39 S. T. Oyama, in *Mechanisms in Homogeneous and Heterogeneous Epoxidation*, ed. S. T. Oyama, Elsevier, Amsterdam, 2008, pp. 1–99.
40 T. A. Nijhuis, M. Makkee, J. A. Moulijn and B. M. Weckhuysen, *Ind. Eng. Chem. Res.*, 2006, **45**, 3447–3459.
41 F. Cavani and J. H. Teles, *ChemSusChem*, 2009, **2**, 508–534.
42 Q. Wang, L. Wang, J. Chen, Y. Wu and Z. Mi, *J. Mol. Catal. A: Chem.*, 2007, **273**, 73–80.
43 V. Duma and D. Hönicke, *J. Catal.*, 2000, **191**, 93–104.
44 A. Held, J. Kowalska-Kuś and K. Nowińska, *Catal. Commun.*, 2012, **17**, 108–113.
45 A. Léonard, J. L. Blin, P. A. Jacobs, P. Grange and B. L. Su, *Microporous Mesoporous Mater.*, 2003, **63**, 59–73.
46 O. A. Anunziata, A. R. Beltramone, M. L. Martínez and L. L. Belon, *J. Colloid Interface Sci.*, 2007, **315**, 184–190.
47 I. Mukherjee, A. Mylonakis, Y. Guo, S. P. Samuel, S. Li, R. Y. Wie, A. Kojtari and Y. Wie, *Microporous Mesoporous Mater.*, 2009, **122**, 168–174.
48 Y. Wie, J. Xu, H. Dong, J. H. Dong, K. Qiu and S. A. Jansen-Varnum, *Chem. Mater.*, 1999, **11**, 2023–2029.
49 J. M. Campelo, D. Luna, R. Luque, J. M. Marinas, A. A. Romero, J. J. Calvino and M. P. Rodríguez-Luque, *J. Catal.*, 2005, **230**, 327–338.
50 C. J. Brinker, *J. Non-Cryst. Solids*, 1988, **100**, 31–50.
51 G. Herrier, J. L. Blin and B. L. Su, *Langmuir*, 2001, **17**, 4422–4430.
52 A. Z. Abdullah, N. Razali and K. T. Lee, *J. Phys. Sci.*, 2010, **21**, 13–27.
53 C. Yu, B. Tian, J. Fan, G. D. Stucky and D. J. Zhao, *J. Am. Chem. Soc.*, 2002, **124**, 4556–4557.
54 K. Flodström, V. Alfredsson and N. Källrot, *J. Am. Chem. Soc.*, 2003, **125**, 4402–4403.
55 J. M. Kim and G. D. Stucky, *Chem. Commun.*, 2000, 1159–1160.
56 B. Naik and N. N. Ghosh, *Recent Pat. Nanotechnol.*, 2009, **3**, 213–224.
57 P. T. Tanev and T. J. Pinnavaia, *Chem. Mater.*, 1996, **8**, 2068–2079.
58 R. Bulánek, L. Čapek, M. Setnička and P. Čičmanec, *J. Phys. Chem. C*, 2011, **115**, 12430–12438.
59 M. S. Kumar, J. Pérez-Ramírez, M. N. Debbagh, B. Smarsly, U. Bentrup and A. Brückner, *Appl. Catal., B*, 2006, **62**, 244–254.